



# The drying process of *Sarcocornia perennis*: impact on nutritional and physico-chemical properties

M. J. Barroca<sup>1,2</sup>  · R. P. F. Guiné<sup>3</sup>  · A. M. Amado<sup>1</sup>  · S. Ressurreição<sup>2</sup>  ·  
A. Moreira da Silva<sup>1,2</sup>  · M. P. M. Marques<sup>1,4</sup>  · L. A. E. Batista de Carvalho<sup>1</sup> 

Revised: 27 February 2020 / Accepted: 24 April 2020  
© Association of Food Scientists & Technologists (India) 2020

**Abstract** The *Sarcocornia* genus is an extreme salt-tolerant plant that can be cultivated in saline habitats almost worldwide. To preserve *Sarcocornia perennis*, convective drying experiments were conducted and their effects on the physico-chemical properties and phenolic content of the plant were studied using conventional and vibrational spectroscopy techniques. The drying process of *Sarcocornia perennis* at temperatures of 40 °C, 50 °C, 60 °C and 70 °C revealed three periods of convective drying process with drying times ranging between 4.5 and 24.9 h, respectively to higher and lower temperatures. The heating-up period can be neglected as compared with the drying process, and the duration of constant rate period, as a percentage of the total drying time, ranged between 34 and 20% respectively at 40 °C and 70 °C. The Modified Page model was proposed to describe the drying process at the different temperatures. From a nutritional point of view, this halophyte plant may be considered as a good source of

fibres, phenolic compounds and natural minerals, such as sodium, potassium, calcium and magnesium. The convective drying, in the temperature range currently used, was found to preserve the colour, nutritional characteristics and phytochemical value of *Sarcocornia perennis*. These results were confirmed by FTIR-ATR and highlight the potential use of the dried plant in novel food products.

**Keywords** Halophyte plants · *Sarcocornia perennis* · Drying process · Kinetic · Physico-chemical properties · FTIR-ATR

## Introduction

The prospect of global warming and freshwater reduction leads to an increase of saline and dry conditions of the land and led to an enhanced need for salt-tolerant crops. Due to their extreme salt tolerance, genera *Salicornia* and *Sarcocornia* (Chenopodiaceae, subfamily Salicornioideae) can be viewed as good candidate plants to be cultivated in saline habitats almost worldwide (Ventura et al. 2011; Ventura and Sagi 2013; Steffen et al. 2015; Flowers and Colmer 2015; García-Caparrós et al. 2017).

*Sarcocornia* (glasswort, samphire) is one of the 16 genera in the Salicornioideae and comprises about 28 succulent species which can be found worldwide, predominantly in warm-temperate and to a lesser extent in subtropical regions (Kadereit et al. 2007; Steffen et al. 2015). *Sarcocornia perennis* is one of the most abundant and representative salt marsh halophytes Mediterranean systems and is characterized by succulent stem without true leaves (de la Fuente et al. 2013; Rufo et al. 2016; Duarte et al. 2018).

**Electronic supplementary material** The online version of this article (<https://doi.org/10.1007/s13197-020-04482-7>) contains supplementary material, which is available to authorized users.

✉ M. J. Barroca  
mjbarroca@gmail.com

- <sup>1</sup> Molecular Physical-Chemistry R&D Unit, Department Chemistry, University of Coimbra, 3004-535 Coimbra, Portugal
- <sup>2</sup> Polytechnic Institute of Coimbra, Coimbra College of Agriculture, Bencanta, 3045-601 Coimbra, Portugal
- <sup>3</sup> CERNAS Research Center and Department of Food Industry, Polytechnic Institute of Viseu, ESAV, Quinta da Alagoa, 3500-606 Viseu, Portugal
- <sup>4</sup> Department of Life Sciences, University of Coimbra, 3000-456 Coimbra, Portugal

The introduction of a diet with non-conventional plant-based foods with nutritional value and functional components is an innovative strategy to diversify and increase food availability. The potential use of the aerial parts of *Salicornia* and *Sarcocornia* species as a vegetable source for human consumption is considered promising, given their high nutritional value in terms of essential nutrients, such as vitamins and natural minerals including Na, Ca, Mg, Fe and K, as well as bioactive compounds such as polyunsaturated fatty acids ( $\alpha$ -linolenic,  $\omega$ 3 and  $\alpha$ -linoleic,  $\omega$ 6), phytosterols, polysaccharides and phenolic compounds. These confer important biological properties, such as antioxidant, anti-inflammatory, hypoglycemic and cytotoxic activity (Jang et al. 2007; Zhu and Row 2010; Ventura et al. 2011; Essaidi et al. 2013; Rodrigues et al. 2014; Isca et al. 2014; Bertin et al. 2016; Costa et al. 2018). The beneficial components of the plants related to their positive effect on human health render *Sarcocornia* a promising functional food, receiving a renewed interest in food and pharmaceutical markets (Patel 2016; Rahman et al. 2018).

*Sarcocornia*'s visually appealing aspect in terms of freshness and colour, coupled to its particular taste, nutritional values and health benefits are attributes that warrant its gourmet status (Ventura et al. 2011). Also, the natural crude extracts and biologically active compounds (such as omega-3 fatty acids, phenolic compounds, antioxidants or minerals) of this halophyte may represent a valuable source for developing a novel food product that satisfies the desires of consumers in terms of health benefits and sensorial acceptance (Costa et al. 2018).

*Sarcocornia* species and the almost identical halophyte plant *Salicornia* have been introduced into the European market as gourmet products with leafless shoots resembling green asparagus. However, their recognition is more widespread in Asian countries, where it is mostly used in fresh salads and pickles (Ventura et al. 2011; Patel 2016). In its dried and milled form, it is used as a herbal salt (Bertin et al. 2016).

*Sarcocornia* and *Salicornia* genus are also well known for their applications as medicinal herbs (Isca et al. 2014) and also in human and domestic animal's diet (Jang et al. 2007).

Fresh halophyte plants are sensitive to microbial spoilage even when refrigerated, thus necessary to freeze or dry them in order to extend their shelf-life. Drying is one of the most widely preservation method, enabling stability at room temperature. Apart from improving the product's shelf-life, this process allows its use as a flavouring, when added or incorporated in other foods. Drying may also be applied as a pretreatment for further processes such as milling (to make powdered products) (Lee and Rhim 2010; Karam et al. 2016). However, the drying process has a

great impact on the plant's structural properties (e.g. shrinkage, porosity, volume, density, pore size distribution, surface area) and also impacts on its physicochemical properties (e.g. texture, colour, nutritive value, appearance) (Zielinska and Markowski 2010; Oikonomopoulou and Krokida 2013; Nguyen et al. 2018; Yang et al. 2020).

Unlike aromatic herbs, halophyte plants have not yet attained the same recognition in the food market, still being underutilised for commercial and human consumption either in fresh or dried state. Despite the increased interest of the food industry in halophytes plants, the reported studies regarding their drying process and its effect on the plant's nutritional qualities is still very scarce. Only one study being found in the literature on several drying processes (conventional air-drying at 45 °C, 60 °C and 75 °C, microwave-drying, microwave-assisted air-drying and freeze-drying) of a perennial halophyte sea fennel (*Crithmum maritimum* L.) and their impact on its properties (Renna et al. 2017). According the study all drying treatments allowed to obtain a water activity lower than 0.537 but reduced the content of essential oils (between 60 and 81%) and chlorophylls (up to 79%) of dried samples. Freeze drying and microwaving preserved the surface colour parameters more than other drying treatments, while freeze-drying gave the best colouring powder. The dried powdered sea fennel obtained with different treatments were added to rice cream to develop a new product, promoting the exploitation of sea fennel.

Different drying methods are used in the drying of vegetables but conventional hot air drying is currently the most widely used method for agricultural products and the changes that occur in the food are mainly affected by drying conditions (Sacilik 2007; Guiné et al. 2012; Arslan and Özcan 2012).

The knowledge of the kinetics of the drying process is pivotal for an accurate understanding of the corresponding mechanism. Furthermore, the influence of variables such as the air temperature, the characteristics of the material and the initial and final moisture contents, on moisture transfer and nutritional value should be evaluated.

Although several studies have been reported on the drying process of various food products, there is still a lack of information regarding the kinetics of the drying process of *Sarcocornia perennis* and its effect on the plant's properties and nutritional benefits. The present work aimed at determining the kinetics of the convective air drying of *Sarcocornia*, in the range of temperatures from 40 to 70 °C, evaluating the effect of the process on the nutritional, physico-chemical and phytochemical characteristics of this halophyte plant. This should contribute to a better exploitation of this species and foster its use in the development of new food products.

## Materials and methods

### Chemicals

Diethyl ether (99.7%), Folin-Ciocalteu's phenol reagent, Kjeldahl selenium catalyst (potassium sulphate 99.9% and selenium 0.1%), methanol (99.5%) and sodium hydroxide (98%) were purchased from PanReac AppliChem (Germany), gallic acid ( $\geq 98\%$ ) and sodium carbonate (99.9%) were obtained from Merck (Germany), while boric acid (99.8%), hydrochloric acid (37%) and sulfuric acid (95–97%) were acquired from Chem-Lab NV (Belgium).

### Biological material

*Sarcocornia perennis* was collected from salt pans in Figueira da Foz— $40^{\circ} 6'42.5627''$  N;  $8^{\circ}49'59.7034''$  W (central region of Portugal), during June 2016. The plants displayed 15–20 cm offshoots. About 250–300 g of 10 cm long samples from the youngest lateral branches and branch tips were used in each drying experiment.

### Experimental drying procedure

The drying kinetics experiments of fresh *Sarcocornia* were performed in a laboratory scale tray dryer (ArmfieldLtd, model UOP8), represented schematically in Fig. 1.

The drying unit consists of a tunnel equipped with heating elements located on the top of the drying unit, and an axial flow fan with adjustable speed yielding a range of air velocities from 0.3 to 1.8 m/s. A power control adjusts the heater power up to 3 kW varying the temperature of the airstream up to 80 °C.

The sample mass was measured continuously with a digital balance OHAUS (Adventurer Pro AV8101), with an

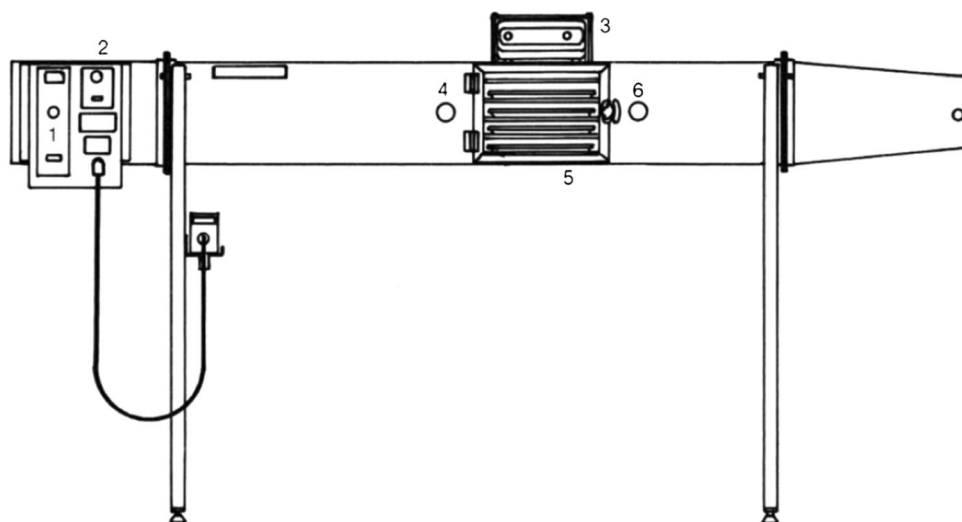
accuracy of 0.1 g, mounted on the top of the dryer body. The sensors of humidity/temperature (HigroClip2 from Rotronic) located upstream and downstream of the drying chamber are external probes of the data logger HygroLog HL-NT3. The ambient humidity and temperature were also measured by a HigroClip2 element. The data from humidity/temperature probes and digital balance were acquired using a HiperTerminal emulator for the connection to a computer.

The velocity of the air at the tunnel outlet was measured with an anemometer (model LCA6000) from Airflow Developments. In order to have a representative value for the velocity, the anemometer was located at each quarter of the tunnel cross-section and the local velocity value was measured. An average value was then calculated to represent a mean value of the air velocity over the entire cross-section at the tunnel outlet. Additional details related with the sketch of the tray dryer as well as the specification and ranges of the measurement devices can be viewed in Castro and Coelho Pinheiro (2016).

The initial moisture content of the samples was determined by weight loss in an oven, at atmospheric pressure and 105 °C until constant weight (AOAC 1997).

For each independent drying experiment, the fan speed and the heat power control were selected to obtain the air conditions (velocity and temperature) required to dry the *Sarcocornia* samples (250–300 g). At the beginning of each experiment, the velocity, temperature and humidity of the airstream, upstream and downstream of the drying chamber, were periodically measured to verify steady-state conditions. Once such conditions were reached, the fresh *Sarcocornia* already in the trays was placed in the drying chamber and its weight was recorded every 40 s. The air conditions were also measured during the drying process, with a view to confirm that the airstream humidity was

**Fig. 1** Sketch of the tray dryer (ArmfieldLtd, model UOP8). (1) Fan speed controller; (2) heater power controller; (3) balance; (4) upstream location of the humidity/temperature sensor; (5) drying chamber (trays); (6) downstream location of the humidity/temperature sensor (Castro and Coelho Pinheiro 2016)



virtually constant and to determine its average value. Table 1 comprises the mean values of the airstream drying parameters, measured upstream and downstream of the drying chamber during the experiments.

Each drying experiment was stopped when the sample weight remained constant for at least half an hour, indicating that the equilibrium moisture was reached.

### Moisture content and drying rate curve

Using the recorded weight of wet *Sarcocornia* during the drying process, the moisture content of the sample ( $X$ ), at each temperature, was obtained in a dry basis

$$X = \frac{W - W_s}{W_s} \quad (1)$$

where  $W$  represents the weight of the whole sample at instant  $t$  and  $W_s$  is the weight of the solids present in the initial wet sample (at instant  $t = 0$ ).

The convective drying rate ( $R$ ) was derived from the drying curve through a finite difference method (Mujumdar 2006):

$$R = -\frac{W_s}{A} \frac{dX}{dt} \cong -\frac{W_s}{A} \frac{\Delta X}{\Delta t} \quad (2)$$

where  $A$  is the drying area,  $W_s$  is the weight of the solids present in the initial wet sample,  $X$  is the moisture content of the sample in a dry basis and  $t$  is the time.

Since mass values were collected at every 40 s, a huge quantity of data was obtained during the drying process, which can include random scatter due, for example, to the uncertainty of the digital balance, or the vibration of the tray caused by the airstream (Kemp et al. 2001). To reduce this uncertainty, time intervals of 600 s for a temperature of 40 °C, 400 s for 50 °C and 200 s for 60 °C and 70 °C, were used in Eq. (2).

### Mathematical approach to determine the critical time

The convective drying process is characterized by the existence of two characteristic periods: the constant drying rate period and the falling drying rate process.

Castro and Coelho Pinheiro (2016) proposed a linear equation ( $X = at + b$ ) to fit the constant drying rate period and a third-degree polynomial ( $X = ct^3 + dt^2 + et + f$ ) to fit the falling rate period. By differentiation of the above equations and applying Eq. (2), it was possible to estimate the correspondent convective drying rate for the constant period ( $R_c$ ),

$$R_c = -\frac{W_s}{A} \frac{dX}{dt} = -\frac{W_s}{A} a \quad (3)$$

and for falling rate period ( $R$ ),

$$R = -\frac{W_s}{A} \frac{dX}{dt} = -\frac{W_s}{A} (3ct^2 + 2dt + e) \quad (4)$$

The critical time ( $t_c$ ) that corresponds to the instant where critical moisture ( $X_c$ ) was reached, was obtained when the values of the constant drying rate ( $R_c$ ) and falling rate period ( $R$ ) were equal, resulting in the following equation (Castro and Coelho Pinheiro 2016):

$$t_c = \frac{-2d + \sqrt{4d^2 - 12c(e - a)}}{6c} \quad (5)$$

The transition between both drying rate periods was obtained iteratively by a simple mathematical approach proposed by Castro and Coelho Pinheiro (2016). After obtaining the critical time, the critical moisture content was easily identified.

The final fitted equations  $X(t)$ , obtained after the iterative methodology, were then differentiated and the drying rate of the constant period ( $R_c$ ) and falling rate period ( $R$ ) were calculated using, respectively, Eqs. (3) and (4).

### Mathematical models to describe the drying process

Several models are currently available in the literature to describe the drying process. Although drying-rate curves have to be measured experimentally, they are practical and give sufficiently good results in mathematical modelling of food drying process. The semitheoretical models presented in Table 2 were used to correlate the experimental data obtained during the drying process of *Sarcocornia perennis* at the different drying conditions.

**Table 1** Airstream drying parameters measured during the experiments

Experiment	Upstream the drying chamber		Downstream the drying chamber		Mean air velocity (m/s)
	Temperature (°C)	Relative humidity (%)	Temperature (°C)	Relative humidity (%)	
40 °C	40.88 ± 1.12	21.96 ± 1.01	39.67 ± 0.99	24.16 ± 1.11	1.09 ± 0.03
50 °C	50.80 ± 0.71	19.87 ± 0.41	50.00 ± 0.72	21.87 ± 0.42	1.11 ± 0.02
60 °C	60.13 ± 0.71	8.93 ± 0.44	59.80 ± 0.81	8.46 ± 0.44	1.12 ± 0.01
70 °C	71.03 ± 1.03	5.96 ± 0.35	69.07 ± 1.04	5.94 ± 0.24	1.09 ± 0.02

The moisture ratio (MR) in the model equations represents the dimensionless sample moisture content at time  $t$  defined as (Erbay and Icier 2010):

$$MR = \frac{X - X_e}{X_i - X_e} \quad (6)$$

where  $X_e$  is the equilibrium moisture in the dry sample at the end of the drying experiment (when equilibrium with the surrounding atmosphere was achieved) and  $X_i$  is the initial moisture content of the sample, all expressed in a dry basis ( $\text{g}_{\text{water}}/\text{g}_{\text{dry solid}}$ ).

The nonlinear regression was used to correlate the experimental sets of  $(MR, t)$  obtained in the drying process at different temperatures. The software used was the Sigma Plot (Version 8.0, SPSS, Inc.).

The goodness of the fit for each model was assessed in the light of the coefficient of determination ( $R^2$ ), mean absolute error (MAE), root mean square error (RMSE), sum of square errors (SSE), standard error (SE) and reduced chi-square test ( $\chi^2$ ), which are statistic parameters generally accepted to evaluate the robustness of a model (Guiné and Barroca 2014).

### Nutritional composition

The methodologies of the Association of Official Analytical Chemicals (AOAC 1997) were used to determine chemical properties of the fresh and dried *Sarcocornia* samples, namely moisture content (method 930.04), crude fibre (method 930.10), ashes (method 930.05), crude protein (method 978.04), total lipids (method 930.09) and total carbohydrate. The total carbohydrate content was determined from the difference between 100 and the sum of the percentages of moisture, crude protein, crude fibre, total lipid, and ash contents.

**Table 2** Some semitheoretical kinetic models used to fit the experimental data of *Sarcocornia perennis* drying process (Vega-Gálvez et al. 2009; Erbay and Icier 2010; Guiné et al. 2011)

Model	Equation
Lewis/Newton	$MR = \exp(-kt)$
Page	$MR = \exp(-kt^n)$
Modified page	$MR = \exp[-(kt)^n]$
Henderson and Pabis	$MR = A \exp(-kt)$
Logarithmic	$MR = A \exp(-kt) + B$
Two-terms	$MR = A \exp(-k_0t) + B \exp(-k_1t)$
Wang and Singh	$MR = 1 + k_0t + k_1t^2$
Verma	$MR = A \exp(-k_0t) + (1 - A) \exp(-k_1t)$
Vega-Lemus	$MR = (a + kt)^2$

To accomplish this purpose, the fresh *Sarcocornia* was triturated using a homogenizer and the dried samples were reduced to a powder.

Total lipids were determined according to the Soxhlet extraction methodology for 16 h using diethyl ether as solvent. Total proteins were determined by the Kjeldahl method and calculated using a nitrogen conversion factor of 6.25 (method 978.04). The DosiFibre method was used to determine crude fibre in a digester (VELP Scientifica, Italy). For ashes, the samples were calcinated in a muffle furnace (Induzir, Portugal) at 550 °C for about 5 h. Three replicates were used for each procedure.

Except for the moisture content, which was expressed in fresh weight, all the other results were expressed in terms of dry matter.

Minerals were determined from ashes (ISO 6869:2000) using a spectra flame atomic absorption spectrophotometer (PerkinElmer PinAAcle 900 T, USA) with the exception of the phosphorus which was analysed by spectrophotometry (ISO 6491:1998).

### Colour

The  $L^*$  (lightness),  $a^*$  (green–red) and  $b^*$  (blue–yellowness) colour values of the fresh and dried samples were assessed using a handheld tristimulus colorimeter (Chroma Meter CR-400, Konica Minolta) calibrated with a white standard tile. To determine the colour parameters 35 measurements were performed for each sample, expressed in  $L^*a^*b^*$ .

The total colour change ( $\Delta E$ ) was considered for evaluation of the overall colour difference between a dried sample and the fresh sample (designated with an index 0) defined as (Guiné and Barroca 2012):

$$\Delta E = \sqrt{(L_0^* - L^*)^2 + (a_0^* - a^*)^2 + (b_0^* - b^*)^2} \quad (7)$$

Larger  $\Delta E$  denotes greater colour change from the fresh sample.

### Extraction

The extraction of fresh and dried samples was performed by stirring with methanol (99.5%) for 24 h and with a plant solvent ratio of 1 g (dry basis):10 mL (Kaiser et al. 2013). The extracts were filtered through a Whatman (Grade 4) filter paper and were used to evaluate the total phenolic content.

### Total phenolic content

The content of phenolic compounds were determined following the method described by Gonçalves et al. (2012).



Briefly, 0.125 mL of each sample (extract) was added to 0.5 mL of deionised water and 0.125 mL of Folin-Ciocalteu reagent. After 6 min, 1.25 mL of 7.5% solution of sodium carbonate and 1.0 mL of deionised water were added.

The mixture was left at room temperature, in the dark, for 60 min, and the absorbance was measured at 760 nm in a  $\mu$ Quant MQX200 microplate reader (Biotek, USA) using 24-well microplates. A calibration curve was built from gallic acid samples within the concentration range 10–50  $\mu\text{g/mL}$ . The total amount of phenolic compounds was determined from the calibration curve and expressed in milligrams of gallic acid equivalents (GAE) per gram of extract:

$$\begin{aligned} \text{Absorbance} &= 0.00614 \times \text{Concentration} + 0.051; \\ R^2 &= 0.999 \end{aligned} \quad (8)$$

### FTIR-ATR spectra

The FTIR-ATR spectra were measured using a Platinum ATR single reflection diamond accessory. Spectra were recorded in the mid-IR region, using a Ge on KBr substrate beamsplitter and a liquid nitrogen cooled wide band Mercury Cadmium Telluride (MCT) detector. Spectra were the sum of 128 scans, at  $2 \text{ cm}^{-1}$  spectral resolution and the 3-term Blackman-Harris apodization function was applied. Under these conditions, the accuracy in wave numbers was well below  $1 \text{ cm}^{-1}$ .

### Statistical analysis

To validate the results obtained for the calculated mean values, a comparison of means was performed by an analysis of variance (ANOVA), with the Post-Hoc Tukey Honestly Significant Difference (HSD) test for identification of differences between three or more groups. Tukey's is a statistical test to identify the differences among groups of data and consists of a single multi-step process for comparison, carried out in conjunction with ANOVA. The test identifies where the difference between two mean values is higher than the standard error which could be expected. For comparison between two groups, the T test for independent samples was used. For the statistical analysis was used the software SPSS version 25 (IBM, Inc.) and the level of significance considered was 5% ( $p < 0.05$ ).

## Results and discussion

### Moisture content and drying rate

Biological materials (such as agricultural products) with a high moisture content generally dry with a constant rate

and subsequent falling rate periods, and the drying process stops when the equilibrium is reached. Knowledge of the kinetics of the drying process is essential for the design and selection of optimised drying methodologies. Thus, it is useful to find experimentally, under certain operating conditions, the moisture content ( $X$ ) as a function of time ( $t$ ). The moisture content curve was obtained after computing  $X$  using Eq. (1). The fresh *Sarcocornia* had a moisture content of  $91.72 \pm 0.07\%$ , which corresponded to moisture content in a dry basis ( $X_i$ ) of  $11.09 \pm 0.04 \text{ g}_{\text{water}}/\text{g}_{\text{dry solid}}$ .

Figure 2 illustrates the dry basis moisture content of *Sarcocornia perennis* during the drying experiments at different temperatures. The drying curves revealed the characteristic trend at constant air drying conditions. From the profile of moisture content, three periods of convective drying are clearly evidenced: (1) the preheating period, in which the wet sample adapts itself to the air conditions, (2) the period of constant drying rate and (3) the falling drying rate. The unsteady state period showed in detail in Fig. 2 (inset) was attained in about 10 min for all temperatures tested, which corresponds to a very short period relative to the overall drying time (lower than 4% under all experimental conditions). This timelag could then be neglected.

After the preheating period, the moisture content of the samples at different temperatures decreased linearly with time ( $R^2 > 0.95$ ) during the constant rate period. For higher drying times, the decrease in the moisture content was slower, indicating a falling drying rate period.

The iterative methodology described above (and detailed in Castro and Coelho Pinheiro (2016)) was applied to determine the instant in which the characteristic periods change. The data of the first period was fitted with a linear function while the second period was fitted to a third-degree polynomial function. Afterwards, the corresponding critical moisture content ( $X_c$ ) was obtained from the drying rate curve to  $t_c$  (Table 3).

After drying time, the moisture content of the *Sarcocornia* sample remained constant and equilibrium with the surrounding atmosphere was achieved.

As expected, there was an acceleration of the drying process due to the increase of air drying temperature from 40 to 70 °C. The drying process at 70 °C allowed a reduction of about 82% of the drying time as compared with the temperature of 40 °C.

Figure 3 presents the drying rate curves of *Sarcocornia perennis* calculated directly from the values measured during the drying experiment at each temperature, and the predicted drying rate curves obtained from the moisture content using Eq. (3) to constant drying period and Eq. (4) to falling drying period. As observed, the drying rate curve that resulted from the application of the mathematical approach is very similar to the experimental drying curve.

**Fig. 2** Moisture content for the convective drying of *Sarcocornia perennis* at temperatures of 40 °C, 50 °C, 60 °C and 70 °C and an air velocity of 1.1 m/s. Inset—detail of the moisture content profile during the unsteady state period, in which the sample adjusts its temperature to the airstream conditions

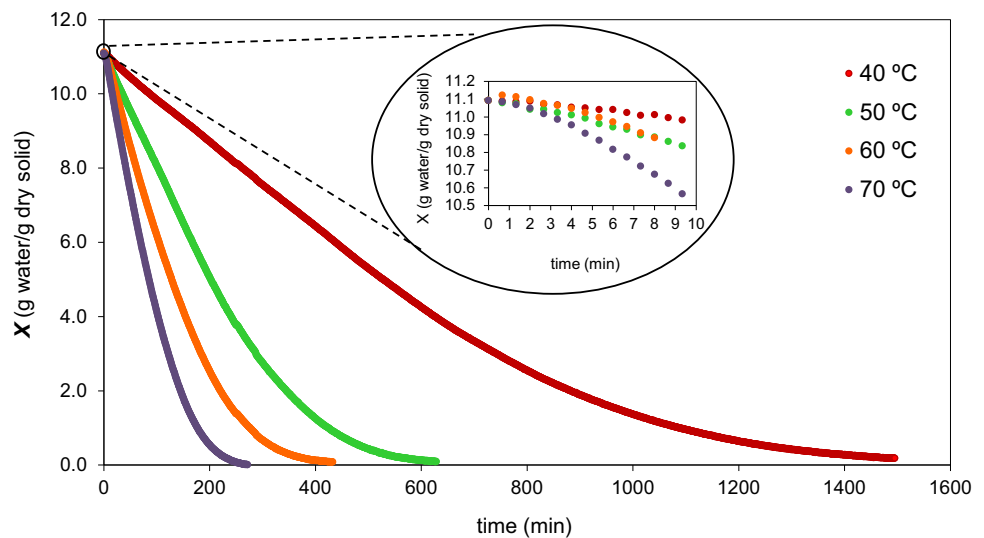


**Table 3** Values of the moisture content of *Sarcocornia perennis*, ( $X$ ), and critical and drying times ( $t_c$  and  $t_d$ ) for the drying process at different temperatures

	40 °C	50 °C	60 °C	70 °C
Moisture content ( $\text{g}_{\text{water}}/\text{g}_{\text{dry solid}}$ )				
$X_i$	11.09	11.09	11.09	11.09
$X_c$	5.22	5.89	7.21	7.52
$X_e$	0.18	0.10	0.08	0.01
Time (min)				
$t_c$	506	171	67	53
$t_d$	1495	629	432	270

Furthermore, the transition from the constant rate period to the falling drying rate was easily identified.

The heating-up period ended during the first 10 min for all temperatures and the correspondent moisture content ranged between 10.9 and 10.7  $\text{g}_{\text{water}}/\text{g}_{\text{dry solid}}$ .

After heating-up period, the drying rate remained almost constant until the critical moisture content was obtained. The period time of constant rate decreased with temperature, ending at a critical moisture content of 5.22  $\text{g}_{\text{water}}/\text{g}_{\text{dry solid}}$ , 5.89  $\text{g}_{\text{water}}/\text{g}_{\text{dry solid}}$ , 7.21  $\text{g}_{\text{water}}/\text{g}_{\text{dry solid}}$  and 7.52  $\text{g}_{\text{water}}/\text{g}_{\text{dry solid}}$ , respectively at 40 °C, 50 °C, 60 °C and 70 °C (Table 3), increasing linearly with temperature ( $R^2 = 0.95$ ).

As observed, the drying temperature exerted an effect on the drying rate, since the surface diffusion was the dominant mechanism in the constant rate period (Srikiatden and Roberts 2007). Towards the end of the constant rate period, water within the *Sarcocornia* sample must be transported from the inside of the sample to the surface until the moisture content reaches the critical moisture content value

( $X_c$ ). The values of constant rate were 1.86, 2.37, 7.59 and 9.66  $\text{g}_{\text{water}}/(\text{m}^2 \text{ min})$ , respectively at 40 °C, 50 °C, 60 °C and 70 °C. The evaporation rate, per unit area of the drying surface, increased with temperature and thus the water at the surface of the sample decreased faster at temperature of 70 °C. Thus, the falling rate period, where the water starts to be transported from the inside of the sample to the surface, began at a higher value of moisture content for the higher temperatures.

After the critical moisture content, the evaporation started to decrease with the moisture content in the sample during the drying process and the evaporation rate became zero reaching the equilibrium moisture content ( $X_e$ ) of 0.18 and 0.01  $\text{g}_{\text{water}}/\text{g}_{\text{dry solid}}$ , respectively, at 40 °C and 70 °C. At this level of moisture, *Sarcocornia* reached a safe moisture level in order to extend its storage life.

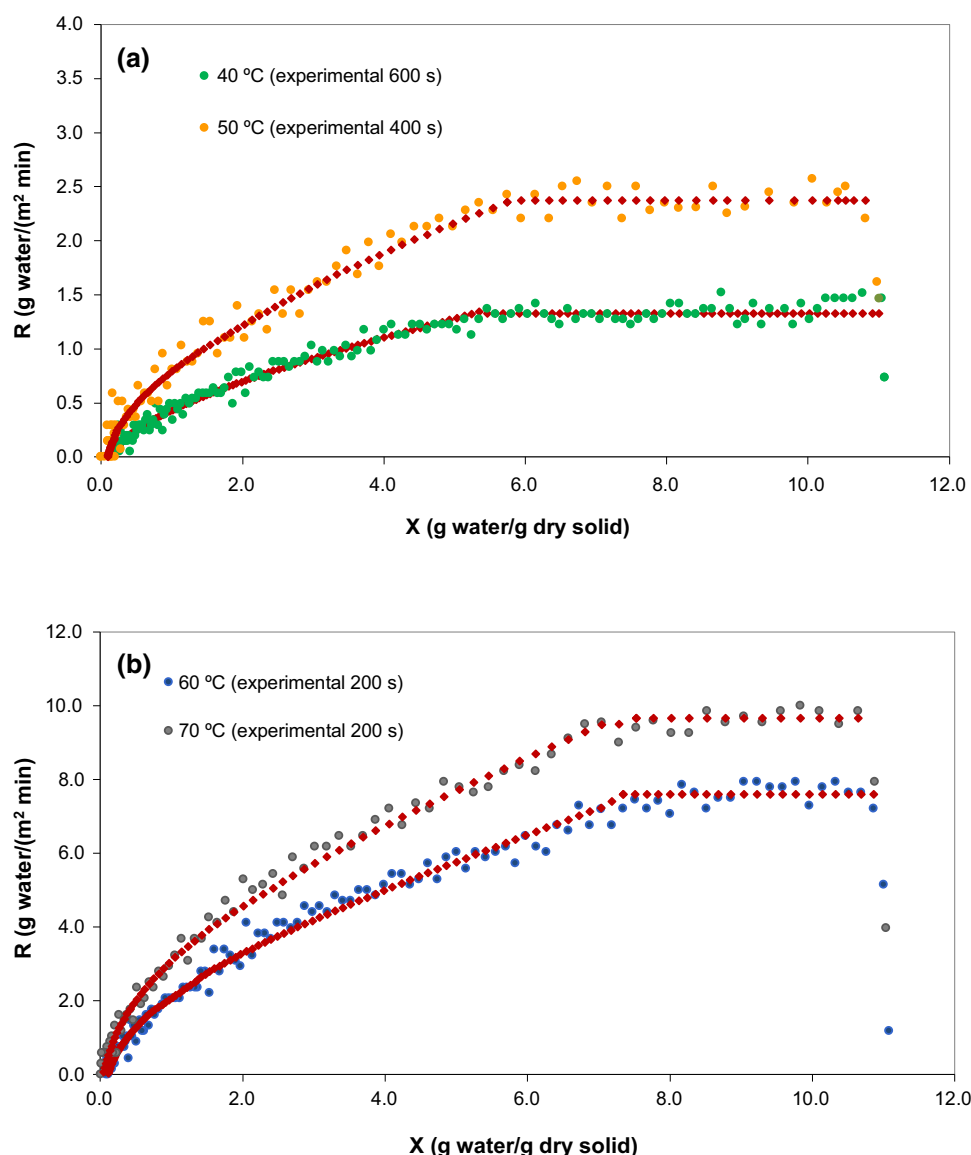
### Mathematical modelling

The lack of physical transport parameters needed to apply the theoretical models at convective drying processes rendered the semitheoretical models as a popular approach during recent decades to describe the convective drying process information. Although drying-rate curves have to be measured experimentally, they are practical and give sufficiently good results in mathematical modelling of food drying.

In order to model the drying process of food products or plants, it is often sufficient to use semitheoretical models which can adequately describe the kinetics of the drying process when the external resistance to heat and mass transfer is eliminated or minimized.

According to Roberts et al. (2008) a convective hot air equal to or greater than 1 m/s and air temperatures between 50 and 70 °C render the external resistance negligible.

**Fig. 3** Drying rate curve for the drying experiments of *Sarcocornia perennis* at 40 °C and 50 °C (a) and 60 °C and 70 °C (b). The symbol  $\blacklozenge$  represents the predicted rate curve obtained from the mathematical approach proposed by Castro and Coelho Pinheiro (2016)



Thus, the air velocity used in this study was 1.1 m/s for insuring negligible external resistance to mass transfer.

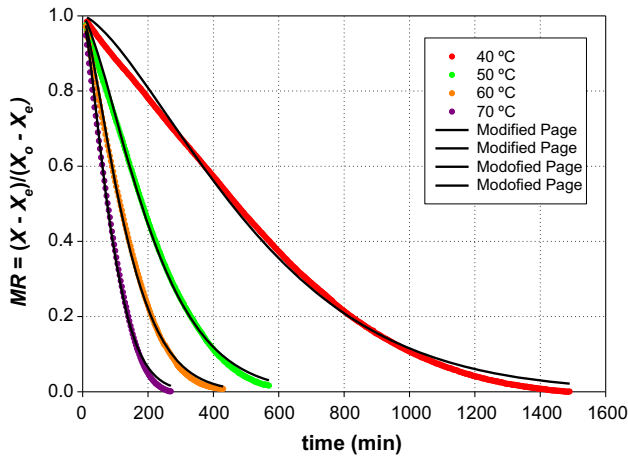
Several models are presently available in the literature to describe the drying process. In order to provide the optimum model parameter estimation, a nonlinear regression was used to correlate the experimental sets of  $(MR, t)$  obtained at different temperatures. To help choose the most adequate model, from the nine tested, the statistical coefficients were calculated. A better fit was obtained for higher values of  $R^2$ , whereas values of  $\chi^2$  and RMSE approaching zero, indicating that the prediction was closer to the experimental data.

Figure 4 shows the  $MR$  data plotted versus  $t$  as well as the results of the regression performed with the best level of correlation (Modified Page model), while Table 4 comprises the model parameters ( $k$  and  $n$ ) and the

corresponding statistical coefficients. Additional details about statistical parameters of the tested models are provided as Supplementary Material.

In general, the Modified Page model presented a good fit for temperatures of 50 °C, 60 °C and 70 °C, along the entire drying periods and with correlation coefficients ranging from 0.9973 to 0.9984. However, when the drying rate was lower, as is the case at 40 °C, the model tended to give higher predictions of the dimensionless moisture ratio for the constant rate period and final drying stage and the fit presented a lower correlation coefficient (0.9962). Thus, the modified Page model appears to be the most suitable for the description of the whole drying process, although for the lower drying air temperature of 40 °C the model presented some difficulty to describe the considerably longer constant rate period.





**Fig. 4** Experimental moisture ratio for the drying experiments of *Sarcocornia perennis* at 40, 50, 60 and 70 °C, and predicted drying curves according to the Modified Page model

However, the Modified Page model showed a global good agreement between predicted and experimental values obtained for the different experiments, indicating that model could be used to calculate the drying of *Sarcocornia* between 40 and 70 °C.

The ability of the Modified Page model to explain the drying pattern of *Sarcocornia* was consistent with other results reported in the literature, showing that the model is also the most suitable one to describe the drying curves of a wide variety of food products like fruits, vegetables, herbs and spices, aromatic plants and meat (Vega et al. 2007; Doymaz 2013; El-Sebaai and Shalaby 2013; Delgado et al. 2014; Khanlari et al. 2014; Calín-Sánchez et al. 2015; Sansaniwal and Kumar 2015; Li et al. 2016).

Furthermore, the drying constant (*k*) obtained from this model increased linearly with temperature for the entire range of temperatures tested:

$$k = 0.000280 \times T(C) - 0.00965; \quad R^2 = 0.995$$

The constant rates of the Modified Page model showed a similar behavior during the drying process of Amasya apple in a laboratory-scale tunnel dryer, between 45 and 85 °C (Yucel et al. 2010). As a result of the important effect of temperature on the drying process, this parameter increased six times when the temperature was raised from 40 to 70 °C. In fact, drying at higher temperatures results in higher moisture diffusivity values and a larger driving force for heat and mass transfer than at lower temperatures (Khanlari et al. 2014; Michailidis and Krokida 2015; Ahmed 2018; Dhali and Datta 2018).

### Nutritional composition and mineral profile of fresh *Sarcocornia*

The moisture content represented the largest single component of *Sarcocornia perennis* (91.72 g/100 g<sub>edible portion</sub>), followed by ash, total carbohydrate, protein, crude fiber and lipids. In general, the nutritional value of the *Sarcocornia perennis* was similar to that of the population of *Sarcocornia ambigua* (Bertin et al. 2014). However, the higher values of ash in *Sarcocornia perennis* (3.83 g/100 g<sub>edible portion</sub>), compared with *Sarcocornia ambigua* (2.96 g/100 g<sub>edible portion</sub>), may be related with their content in minerals. The major minerals found to *Sarcocornia perennis* were Na (13.7 mg/g fresh matter), K (1.0 mg/g fresh matter), Ca (0.89 mg/g fresh matter), Mg (0.3 mg/g fresh matter) and P (0.2 mg/g fresh matter) followed by Fe (20.8 µg/g fresh matter), Mn (4.1 µg/g fresh matter), Zn (2.5 µg/g fresh matter) in minor levels. From a nutritional point of view, this halophyte plant may be considered as a good source of minerals, such as sodium, phosphorous, calcium and magnesium. The intake of 100 g of fresh *Sarcocornia perennis* corresponds, respectively, to 57%, 20%, 89% and 75% of the daily values recommended per day of sodium, phosphorous, calcium and magnesium

**Table 4** Modified Page model parameters and values of statistical coefficients for the drying process of *Sarcocornia perennis* at 40, 50, 60 and 70 °C and air velocity of 1.1 m/s

Parameters	40 °C	50 °C	60 °C	70 °C
<i>k</i> (± sd)	0.0017(± 4.1950 × 10 <sup>-6</sup> )	0.0043(± 1.2083 × 10 <sup>-5</sup> )	0.0068(± 2.0958 × 10 <sup>-5</sup> )	0.0102(± 5.0151 × 10 <sup>-5</sup> )
<i>n</i> (± sd)	1.4403(± 0.0077)	1.3973(± 0.0084)	1.3589(± 0.0086)	1.4069(± 0.0146)
<i>R</i> <sup>2</sup>	0.9962	0.9980	0.9984	0.9973
MAE	0.0163136	0.0112135	0.0026663	0.0132803
RMSE	0.0186618	0.0131340	0.0113249	0.0147214
SSE	0.0003483	0.0001725	0.0001283	0.0002235
SE	0.0008837	0.0010073	0.0010010	0.0016512
χ <sup>2</sup>	0.0003498	0.0001745	0.0001303	0.0002205

sd standard deviation

(FDA 2016; EFSA 2017). The variations in the chemical composition of *Sarcocornia* species in different countries can be due to their different soil and water conditions, particularly the salinity.

### Effect of the drying process on the nutritional profile, total phenolic content and colour of dried *Sarcocornia*

The moisture content of dehydrated *Sarcocornia* powder ranged from 10.67 g/100 g<sub>fresh matter</sub> and 4.49 g/100 g<sub>fresh matter</sub>, respectively at 40 °C and 70 °C.

Table 5 shows the average values of the main chemical components for dehydrated *Sarcocornia* powder after the drying experiments (on dry basis).

In general, the nutritional profile of dehydrated *Sarcocornia perennis*, at different temperatures, was undifferentiated, meaning that the nutritional composition of the dehydrated plant was not very much affected by the drying process for the range of temperatures studied. Therefore, drying may be a good process of preservation without loss of the plant's nutritive value, in the temperature interval tested. Tanongkankit et al. (2012) also concluded that oven drying at 60 °C, 70 °C and 80 °C did not result in any significant effect on the chemical composition of functional dietary fiber powder produced by cabbage outer leaves.

Phenolic compounds from plants constitute one of the major groups of compounds acting as primary antioxidants and, therefore, measurement of the total phenolic content in fresh and dried halophyte extracts can be used to assess their antioxidant properties. The amount of phenolic compounds in *Sarcocornia* was measured, yielding the values:  $29.05 \pm 0.51$ ,  $29.35 \pm 0.27$  and  $27.40 \pm 0.32$  mg GAE/g extract, respectively for fresh and dried samples (at 40 °C and 70 °C). Kumari and Khatkar (2018) argued that the slight reduction in phenolic compounds in the plant dehydrated at 70 °C might be due to the conversion of the polyphenols into other forms. According to Kyi et al. (2005), the reactions involved in the decrease of polyphenolic compounds with increasing drying temperature (40–60 °C) are associated to enzymatic and non-enzymatic oxidation reactions. However, even at the higher drying temperature currently used (70 °C), the phenolic content in fresh and dried *Sarcocornia* are negligibly different. Thus, the use of these halophytes in the dry state instead of fresh can be a good alternative when developing products such as natural salt substitutes, enriched with antioxidant compounds.

As shown in Table 5 the  $L^*$ ,  $a^*$  and  $b^*$  colour coordinates for fresh *Sarcocornia perennis* were  $33.83 \pm 2.61$ ,  $-12.27 \pm 1.48$  and  $16.09 \pm 2.16$ , respectively.

Comparing the colour parameters of the dried samples with those obtained for fresh *Sarcocornia*, it was possible

to conclude that drying induced a rise in  $L^*$  colour parameters indicating an increase in the lightness of dehydrated plant. However, parameter  $L^*$  was higher at lower temperature than at higher temperatures, indicating that the samples dried at 40 °C presented a lighter colour than the ones dried at higher temperatures.

A negative  $a^*$  value, which represents green colour, increased after drying and, consequently dried plant presented a lesser intensity of the green colour than the fresh ones. However, the greenness parameter ( $a^*$ ) was three times higher at 40 °C than for the samples dried at 70 °C, suggesting that the latter preserved the green intensity better. The increase of  $a^*$  parameter values after convective drying was also reported for many green vegetables and plants such as pepper (Guiné and Barroca 2012) and *Allium roseum* leaves (Said et al. 2013).

The mechanisms involved in chlorophyll degradation include the loss of the phytol group through the action of the enzyme chlorophyllase. Therefore, the higher temperatures could promote the inactivation of chlorophyllase with the minimal conversion of chlorophyll to pheophytin (Heaton and Marangoni 1996). Furthermore, during heat treatments, some mechanisms related with chlorophyll and other pigments decomposition and conversion of some non-coloured and less coloured precursors of green colour into more visible green colour can occur simultaneously, depending on temperature and time (van Boekel 1999, 2000; Tijssens et al. 2001; Lu et al. 2010).

The total colour difference ( $\Delta E$ ), which is a combination of the  $L^*$ ,  $a^*$  and  $b^*$  values, is a colour parameter extensively used to characterize the total variation of colour in food during processing. As observed in Table 5, the colour difference parameter decreased linearly with temperature ( $R^2 = 0.92$ ). Colour pigments are sensitive to enzymatic and non-enzymatic browning and other degradation reactions during drying. Although the increase of temperature leads to an increase of reaction rates, temperatures from 50 to 80 °C can lead to their inactivation, reducing considerably the enzymatic reactions with temperature and consequently the colour degradation (Martylenko and Bück 2019). Moreover, during the drying experiments the samples were in contact with oxygen that promotes the non-enzymatic browning and pigment oxidation. Hence, for the higher heating temperature of 70 °C the samples were in contact with the airstream during much less time (4.5 h) than at 40 °C (24.9 h) which originated a lesser total degradation of pigments. Thus, the drying process of *Sarcocornia* at a higher temperature but with much less drying time originated less intense colour changes in dried plant. These findings are in agreement with Yuan et al. (2015) who suggested that oven drying chrysanthemum flower at 70 °C was the most appropriate post-harvest processing method to obtain final products with higher levels of

**Table 5** Nutritional composition (g per 100 g of dry matter), polyphenols content (mg GAE/g extract) and colour of fresh and dried *Sarcocornia perennis*

	Fresh	40 °C	50 °C	60 °C	70 °C	Statistics all <sup>1</sup> N, F, <i>p</i> value	Statistics only dried <sup>2</sup> N, F, <i>p</i> -value
<i>Nutritional</i>							
Crude protein	15.60 ± 0.03 <sup>a</sup>	18.26 ± 0.12 <sup>cβγ</sup>	17.61 ± 0.33 <sup>cβ</sup>	16.56 ± 0.07 <sup>bα</sup>	18.98 ± 0.11 <sup>dγ</sup>	3, 125.698, < 0.0005	3, 59.146, 0.001
Total lipids	1.37 ± 0.07 <sup>a</sup>	2.48 ± 0.16 <sup>bα</sup>	2.83 ± 0.09 <sup>bα</sup>	2.76 ± 0.16 <sup>bα</sup>	2.48 ± 0.01 <sup>bα</sup>	3, 54.920, < 0.0005	3, 4.558, 0.088
Crude fiber	8.63 ± 0.15 <sup>a</sup>	10.89 ± 0.02 <sup>cβ</sup>	10.65 ± 0.07 <sup>cβ</sup>	9.39 ± 0.20 <sup>bα</sup>	9.47 ± 0.10 <sup>bα</sup>	3, 116.251, < 0.0005	3, 89.120, < 0.0005
Ash	43.62 ± 0.05 <sup>a</sup>	45.30 ± 0.17 <sup>bα</sup>	43.94 ± 1.47 <sup>αα</sup>	43.88 ± 0.09 <sup>αα</sup>	45.71 ± 0.13 <sup>αα</sup>	3, 4.028, 0.079	3, 3.159, 0.148
Total carbohydrate <sup>4</sup>	30.80 ± 0.19 <sup>c</sup>	23.09 ± 0.43 <sup>αα</sup>	24.98 ± 1.78 <sup>bβαβ</sup>	27.42 ± 0.06 <sup>bβ</sup>	23.37 ± 0.11 <sup>αα</sup>	3, 30.361, 0.001	3, 9.350, 0.028
Polyphenols <sup>3</sup>	29.05 ± 0.51 <sup>ab</sup>	29.35 ± 0.27 <sup>b</sup>	nd	nd	27.40 ± 0.32 <sup>a</sup>	3, 12.741, 0.034	3, 5.408, 0.033 <sup>4</sup>
<i>Colour</i>							
L	33.83 ± 2.61 <sup>a</sup>	51.33 ± 2.53 <sup>εδ</sup>	47.94 ± 1.39 <sup>dγ</sup>	45.71 ± 1.31 <sup>cβ</sup>	43.57 ± 2.20 <sup>bα</sup>	35, 323.949, < 0.0005	35, 103.207, < 0.0005
a*	– 12.27 ± 1.48 <sup>a</sup>	– 2.72 ± 0.27 <sup>εδ</sup>	– 6.44 ± 0.47 <sup>cβ</sup>	– 5.99 ± 0.34 <sup>dγ</sup>	– 8.17 ± 0.40 <sup>bα</sup>	35, 778.312, < 0.0005	35, 1264.168, < 0.0005
b*	16.09 ± 2.16 <sup>a</sup>	20.91 ± 0.48 <sup>bα</sup>	26.32 ± 0.71 <sup>dγ</sup>	27.75 ± 0.72 <sup>εδ</sup>	25.39 ± 0.51 <sup>cβ</sup>	35, 594.006, < 0.0005	35, 625.144, < 0.0005
ΔE	0	20.56 ± 2.14 <sup>γ</sup>	18.41 ± 1.11 <sup>β</sup>	17.84 ± 0.97 <sup>β</sup>	14.16 ± 1.81 <sup>α</sup>	–	35, 98.958, < 0.0005

<sup>1</sup>Comparison between all samples, i.e., fresh and dried at different temperatures. Mean values in the same line with the same Arabic superscript are not statistically different according to ANOVA with post-hoc test Tukey at a 95% confidence level (*p* < 0.05); N = number of measurements, F = test statistic, *p* value = significance

<sup>2</sup>Comparison between the dried samples alone. Mean values in the same line with the same Greek superscript are not statistically different according to ANOVA with post-hoc test Tukey at 95% confidence level (*p* < 0.05); N = number of measurements, F = test statistic, *p* value = significance

<sup>3</sup>Test T for independent samples at 95% confidence level (*p* < 0.05), for comparison of two groups

<sup>4</sup>Calculated by difference

nd not determined

bioactive ingredients in a small amount of time, in the range of temperatures from 40 to 120 °C.

### FTIR-ATR analysis of dried *Sarcocornia*

Fourier-transform infrared spectroscopy (FTIR-ATR) is a powerful spectroscopic technique that can be used for both quantitative and qualitative analysis, as the output is a detailed information about the chemical composition of the samples. FTIR is an appealing technique within the food industry because it is simple, rapid, non-destructive and very accurate, allowing to discriminate even very similar compounds from a small amount of sample (Liang et al. 2013). Thus, the FTIR-ATR spectra of fresh and dried *Sarcocornia* at 40 °C and 70 °C was also obtained to provide information on the fundamental vibrational modes of the sample components that translate into a set of bands, which are correlated with specific functional groups (and therefore function), as a unique fingerprint of each molecule.

Figure 5 contains FTIR-ATR spectra of fresh and dried (at 40 °C) *Sarcocornia perennis*, in the 750–4000  $\text{cm}^{-1}$  spectral region. As expected, the bands were generally broad, causing a strong overlap. The most prominent spectral profile, which spreads across the 2700–3700  $\text{cm}^{-1}$  region, was correlated with the O–H elongation ( $\nu\text{OH}$ ) (Carey 1982; Heredia-Guerrero et al. 2014). Its high intensity denotes the presence of a high amount of water. However, other biochemical constituents also contributed to this spectral interval, namely carbohydrates, phenolic compounds and non-esterified fatty acids (Stuart 1997).

The two well-defined signals centered at 2849 and 2916  $\text{cm}^{-1}$  measured for fresh *Sarcocornia* (Fig. 5a) were associated with the symmetric and antisymmetric  $\text{CH}_2$  group stretching modes ( $\nu_s\text{CH}_2$  and  $\nu_{as}\text{CH}_2$ ), mainly from fatty acids (Heredia-Guerrero et al. 2014; Poiana et al. 2015). The presence of  $\text{CH}_3$ -groups was denoted by the low-intensity shoulders detected on both wings of the band centered at 2916  $\text{cm}^{-1}$  (at ca. 2895 and 2954  $\text{cm}^{-1}$ , ascribed to the symmetric ( $\nu_s\text{CH}_3$ ) and antisymmetric ( $\nu_{as}\text{CH}_3$ ) stretching modes, respectively) (Heredia-Guerrero et al. 2014; Poiana et al. 2015).

Upon drying at 40 °C, the expected significant intensity decreases of the  $\nu\text{OH}$  intensity emphasizes a weak shoulder at ca. 3014  $\text{cm}^{-1}$  (Fig. 5b), that was ascribed to the C–H stretching modes in the  $-\text{CH}=\text{CH}-$  moieties of unsaturated fatty acids. This result suggested the presence of a significant amount of unsaturated fatty acids in the plant, in line with reported results on other *Sarcocornia* species (Costa et al. 2014).

In addition, the presence of carbonyl-containing compounds in the samples was reflected in the relatively broad band with an absorbance maximum at 1734  $\text{cm}^{-1}$ . This

spectral feature was assigned to the C=O stretching mode ( $\nu\text{C}=\text{O}$ ) of the cutin constituents of the plant, such as esters and carboxylic acids (Heredia-Guerrero et al. 2014). The involvement of these constituents in hydrogen bonding interactions (either strong or weak) leads to different chemical environments, justifying the broad profile of the band.

Immediately following, on the lower frequency side, appeared another relatively broad spectral feature with a maximum of absorption at 1637  $\text{cm}^{-1}$ . Part of the considerable intensity absorption of this band was due to the contribution of the deformation mode H–O–H of the water ( $\delta\text{H}_2\text{O}$ ) that broadens the overall profile to the band at 1734  $\text{cm}^{-1}$  and obscures other less intense bands (Fan et al. 2012). Removing water from the sample leads to a reduction of the band associated to the  $\delta\text{H}_2\text{O}$ , allowing the appearance of other low-intensity bands that were hidden (e.g. 1493 and 1517  $\text{cm}^{-1}$ ). At the same time, the band absorption maximum was shifted downward to 1617  $\text{cm}^{-1}$ , turning the band profile around 1734  $\text{cm}^{-1}$  better defined (Fig. 5b).

The main spectral profile (with maximum at 1617  $\text{cm}^{-1}$ ) after drying comprised the bands due to the conjugation between the stretching modes associated to the aromatic CC bonds ( $\nu\text{CC}_{\text{ring}}$ ) and non-aromatic C=C stretching modes ( $\nu\text{C}=\text{C}$ ) (Heredia-Guerrero et al. 2014). These bands may be used for the composition analysis of the extracts regarding the content of aromatic compounds, namely phenolic acids and other type of components, and unsaturated non-aromatic components, such as unsaturated fatty acids. Several other spectral features were observable at lower frequencies. However, their relation to a specific group of components was not so straightforward as they were mainly ascribed to modes related to molecular groups common to most of the organic compounds, namely skeletal C–C and C–O stretching modes ( $\nu\text{CC}$  and  $\nu\text{CO}$ , respectively) and C–O–C, C–C–H, C–C–O and C–O–H deformation modes ( $\delta\text{COC}$ ,  $\delta\text{CCH}$ ,  $\delta\text{CCO}$  and  $\delta\text{COH}$ , respectively) (Fan et al. 2012). These observations show that FTIR-ATR spectroscopy can yield valuable information regarding potential changes on the moisture and biochemical composition of *Sarcocornia* samples due to drying.

Figure 5 also compared the FTIR-ATR spectra recorded for *Sarcocornia* samples submitted to drying procedures (temperature-dried at 40 °C and 70 °C) with the spectrum obtained for fresh samples in two particularly sensitive spectral regions, namely 1500–1800  $\text{cm}^{-1}$  (Fig. 5c) and 2700–3700  $\text{cm}^{-1}$  (Fig. 5d). As stated above these spectral regions included the bands associated with some vibrational modes of water and were therefore sensitive to drying.

The analysis of the whole spectral regions showed that both the  $\nu\text{OH}$  and  $\delta\text{H}-\text{O}-\text{H}$  related bands have an equally significant intensity decrease regardless of the drying

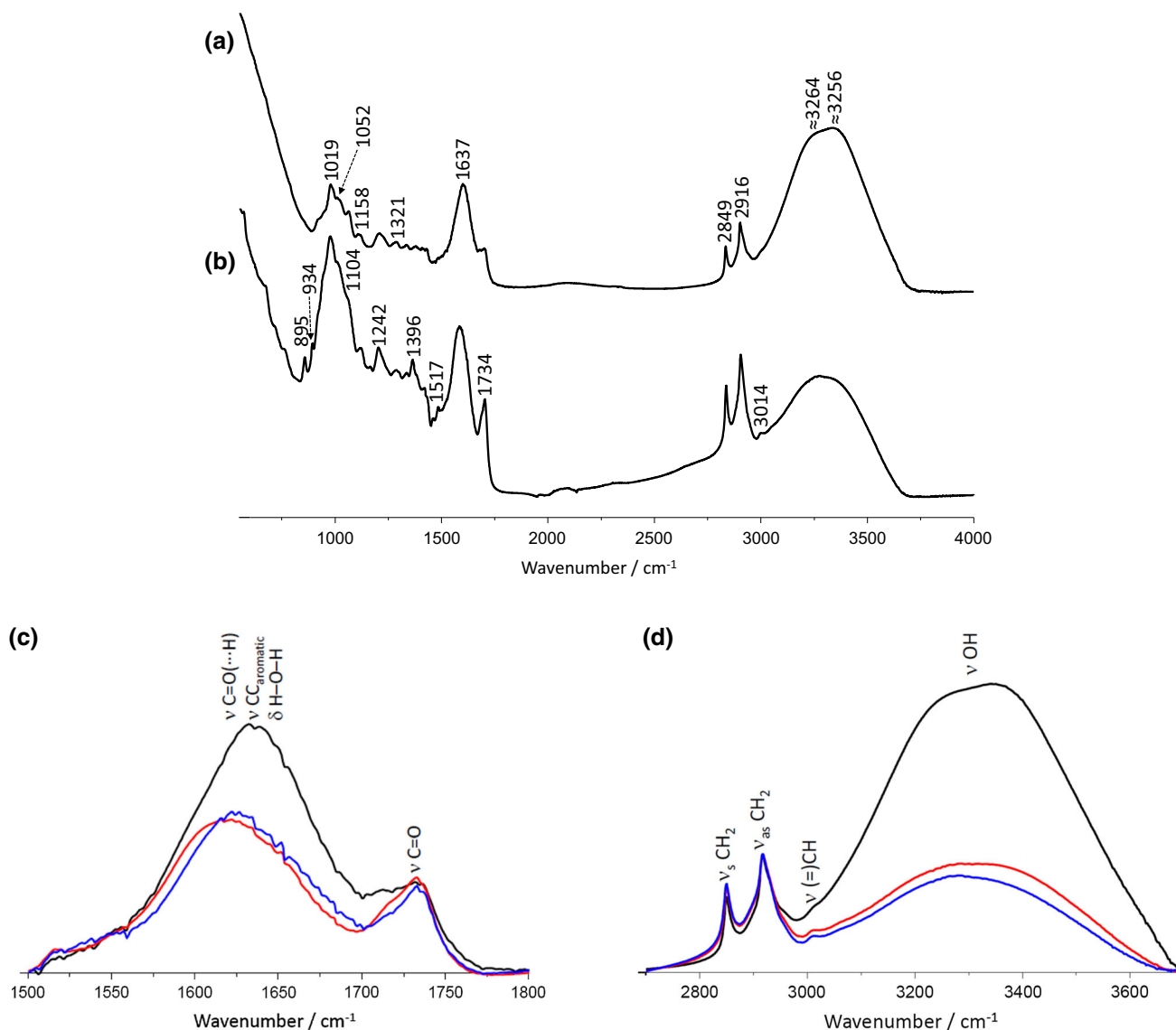


**Fig. 5** FTIR-ATR spectra (750–4000 cm<sup>-1</sup>) of fresh (a) and dried (at 40 °C) (b) *Sarcocornia perennis*. FTIR-ATR spectra of fresh (black) and dried *Sarcocornia* samples (40 °C (red) and 70 °C (blue)), in the 1500–1800 cm<sup>-1</sup> (c) and 2700–3700 cm<sup>-1</sup> (d) regions

procedure adopted. These results are in line with the composition characterization obtained previously, suggesting that most of the moisture was removed even at 40 °C. Also supporting the biochemical results, the analysis of the two spectral regions suggested that the composition in lipids and aromatic compounds, notably phenolic, was not significantly altered even when drying was carried out at temperatures up to 70 °C.

## Conclusion

The drying process of *Sarcocornia perennis* revealed three periods of convective drying process (pre-heating, constant rate and falling rate) with time intervals from 4.5 and

24.9 h, respectively for higher and lower temperatures. The heating-up period can be neglected as compared with the drying process, and the duration of constant rate period, as a percentage of the total drying time, ranged between 34 and 20% respectively at 40 °C and 70 °C.

Moreover, the critical moisture content correlated linearly with temperature ( $R^2 = 0.95$ ). From the mathematical models tested, the Modified Page model was found to be the most suitable to describe the drying process of *Sarcocornia* in the temperature interval tested.

From a nutritional point of view, this halophyte plant may be considered as a good source of fibres, phenolic compounds and natural minerals such as sodium, phosphorous, calcium and magnesium. These findings coupled to FTIR-ATR analysis allowed to confirm that a convective



process between 40 and 70 °C preserved the nutritional value and the phenolic content of the plant.

Taking into account the drying efficiency and the characteristics (nutritional, total phenolic content and colour) of dried *Sarcocornia perennis*, convective drying at 70 °C revealed to be the most appropriate methodology for preserving the health-beneficial properties of the plant.

**Acknowledgements** The authors acknowledge financial support from Project ReNATURE—Valorization of the Natural Endogenous Resources of the Centro Region (Centro 2020, Centro-01-0145-FEDER-000007, IDEAS4life—Novos IngreDiEntes Alimentares de Plantas Marítimas (POCI-01-0145-FEDER-029305) and project CENTRO-01-0145-FEDER-023631: SoSValor. The authors also thank José João Rodrigues for the halophyte supply, and Prof. Jorge Canhoto, R&D Centre of Functional Ecology, University of Coimbra, for the taxonomic identification of the biological material.

## References

- AOAC—Official methods of analysis of AOAC international (1997). 16th edn, vol 1. USA
- Ahmed J (2018) Drying of vegetables: principles and drying design. In: Siddiq M, Uebersax MA (eds) Handbook of vegetables and vegetable processing, 2nd edn. Wiley, New York, pp 381–405
- Arslan D, Özcan MM (2012) Evaluation of drying methods with respect to drying kinetics, mineral content, and color characteristics of savory leaves. Food Bioprocess Technol 5:983–991. <https://doi.org/10.1007/s11947-010-0498-y>
- Bertin RL, Gonzaga LV, Gonzaga LV, Borges GSC, Azevedo MS, Maltez HF, Heller M, Micke GA, Tavares LBB, Fett R (2014) Nutrient composition and identification/quantification of major phenolic compounds in *Sarcocornia ambigua* (Amaranthaceae) using HPLC–ESI-MS/MS. Food Res Int 55:404–411. <https://doi.org/10.1016/j.foodres.2013.11.036>
- Bertin RL, Gonzaga LV, Borges GSC, Azevedo MS, Maltez HF, Heller M, Micke GA, Tavares LBB, Fett R (2016) Mineral composition and bioaccessibility in *Sarcocornia ambigua* using ICP-MS. J Food Compos Anal 47:45–51. <https://doi.org/10.1016/j.jfca.2015.12.009>
- Calín-Sánchez Á, Kharaghani A, Lech K, Figiel A, Carbonell-Barrachina ÁA, Tsotsas E (2015) Drying kinetics and microstructural and sensory properties of black chokeberry (*Aronia melanocarpa*) as affected by drying method. Food Bioprocess Technol 8:63–74. <https://doi.org/10.1007/s11947-014-1383-x>
- Carey PR (1982) Biochemical applications of Raman and resonance Raman spectroscopies. Academic Press, Paris
- Castro LMMN, Coelho Pinheiro MN (2016) A simple data processing approach for drying kinetics experiments. Chem Eng Commun 203:258–269. <https://doi.org/10.1080/00986445.2014.993468>
- Costa CSB, Chaves FC, Rombaldi CV, Souza CR (2018) Bioactive compounds and antioxidant activity of three biotypes of the sea asparagus *Sarcocornia ambigua* (Michx.) M.A. Alonso & M.B. Crespo: a halophytic crop for cultivation with shrimp farm effluent. South Afr J Bot 117:95–100. <https://doi.org/10.1016/j.sajb.2018.05.011>
- Costa CSB, Vicenti JRM, Morón-Villarreyes JA, Caldas S, Cardoso LV, Freitas RF, D'oca MGM (2014) Extraction and characterization of lipids from *Sarcocornia ambigua* meal: a halophyte biomass produced with shrimp farm effluent irrigation. Anais da Academia Brasileira de Ciências 86:935–943. <https://doi.org/10.1590/0001-3765201420130022>
- Dhali K, Datta AK (2018) Experimental analyses of drying characteristics of selected food samples. Agric Eng Int CIGR J 20:188–194
- de la Fuente V, Rufo L, Rodríguez N, Sánchez-Mata D, Franco A (2013) A micromorphological and phylogenetic study of *Sarcocornia* A.J. Scott (Chenopodiaceae) on the Iberian Peninsula. Plant Biosyst Int J Deal All Aspects Plant Biol 147:158–173. <https://doi.org/10.1080/11263504.2012.752414>
- Delgado T, Pereira JA, Baptista P, Casal S, Ramalhosa E (2014) Shell's influence on drying kinetics, color and volumetric shrinkage of *Castanea sativa* Mill. fruits. Food Res Int 55:426–435. <https://doi.org/10.1016/j.foodres.2013.11.043>
- Doymaz İ (2013) Experimental study on drying of pear slices in a convective dryer. Int J Food Sci Technol 48:1909–1915. <https://doi.org/10.1111/ijfs.12170>
- Duarte B, Silva H, Dias JM, Sleimi N, Marques JC, Caçador I (2018) Functional and ecophysiological traits of *Halimione portulacoides* and *Sarcocornia perennis* ecotypes in Mediterranean salt marshes under different tidal exposures. Ecol Res 33:1145–1156
- EFSA (2017) Dietary reference values for nutrients—summary report. European Food Safety Authority. <https://efsa.onlinelibrary.wiley.com/doi/epdf/10.2903/sp.efsa.2017.e15121>. Accessed 31 Jan 2020
- El-Sebaei AA, Shalaby SM (2013) Experimental investigation of an indirect-mode forced convection solar dryer for drying thymus and mint. Energy Convers Manag 74:109–116. <https://doi.org/10.1016/j.enconman.2013.05.006>
- Erbay Z, Icier F (2010) A review of thin layer drying of foods: theory, modeling, and experimental results. Crit Rev Food Sci Nutr 50:441–464. <https://doi.org/10.1080/10408390802437063>
- Essaidi I, Brahmi Z, Snoussi A, Koubaier HBH, Casabianca H, Abe NA, Omri AE, Chaabouni MM, Bouzouita N (2013) Phytochemical investigation of Tunisian *Salicornia herbacea* L., antioxidant, antimicrobial and cytochrome P450 (CYPs) inhibitory activities of its methanol extract. Food Control 32:125–133. <https://doi.org/10.1016/j.foodcont.2012.11.006>
- Fan M, Dai D, Huang B (2012) Fourier transform infrared spectroscopy for natural fibres. In: Salih S (ed) Fourier transform-materials analysis. InTech, Croatia, pp 45–68
- FDA (2016) Food labeling: revision of the nutrition and supplement facts labels. Food and Drug Administration. <https://s3.amazonaws.com/public-inspection.federalregister.gov/2016-11867.pdf>. Accessed 31 Jan 2020
- Flowers TJ, Colmer TD (2015) Plant salt tolerance: adaptations in halophytes. Ann Bot 115:327–331. <https://doi.org/10.1093/aob/mcu267>
- García-Caparrós P, Llanderal A, Pestana M, Correia PJ, Lao MT (2017) Nutritional and physiological responses of the dicotyledonous halophyte *Sarcocornia frutescens* to salinity. Aust J Bot 65:573–581. <https://doi.org/10.1071/BT17100>
- Gonçalves FJ, Rocha SM, Coimbra MA (2012) Study of the retention capacity of anthocyanins by wine polymeric material. Food Chem 134:957–963. <https://doi.org/10.1016/j.foodchem.2012.02.014>
- Guiné RP, Barroca MJ (2014) Quantification of browning kinetics and colour change for quince (*Cydonia oblonga* Mill.) exposed to atmospheric conditions. Agric Eng Int CIGR J 16:285–298
- Guiné RP, Pinho S, Barroca MJ (2011) Study of the convective drying of pumpkin (*Cucurbita maxima*). Food Bioprod Process 89:422–428
- Guiné RPF, Barroca MJ (2012) Effect of drying treatments on texture and color of vegetables (pumpkin and green pepper). Food Bioprod Process 90:58–63. <https://doi.org/10.1016/j.fbp.2011.01.003>

- Guiné RPF, Henriques F, Barroca MJ (2012) Mass transfer coefficients for the drying of pumpkin (*Cucurbita moschata*) and dried product quality. *Food Bioprocess Technol* 5:176–183. <https://doi.org/10.1007/s11947-009-0275-y>
- Heaton JW, Marangoni AG (1996) Chlorophyll degradation in processed foods and senescent plant tissues. *Trends Food Sci Technol* 7:8–15. [https://doi.org/10.1016/0924-2244\(96\)81352-5](https://doi.org/10.1016/0924-2244(96)81352-5)
- Heredia-Guerrero JA, Benítez JJ, Domínguez E, Bayer IS, Cingolani R, Athanassiou A, Heredia A (2014) Infrared and Raman spectroscopic features of plant cuticles: a review. *Front Plant Sci*. <https://doi.org/10.3389/fpls.2014.00305>
- Isca VMS, Seca AML, Pinto DCGA, Silva H, Silva AMS (2014) Lipophilic profile of the edible halophyte *Salicornia ramosissima*. *Food Chem* 165:330–336. <https://doi.org/10.1016/j.foodchem.2014.05.117>
- Jang H-S, Kim K-R, Choi S-W, Woo M-H, Choi J-H (2007) Antioxidant and antithrombus activities of enzyme-treated *Salicornia herbacea* extracts. *Ann Nutr Metab* 51:119–125. <https://doi.org/10.1159/000100826>
- Kadereit G, Ball P, Beer S, Mucina L, Sokoloff D, Teege P, Yaprak AE, Freitag H (2007) A taxonomic nightmare comes true: phylogeny and biogeography of glassworts (*Salicornia* L., Chenopodiaceae). *Taxon* 56:1143–1170. <https://doi.org/10.2307/25065909>
- Kaiser S, Verza SG, Moraes RC, Pittol V, Peñaloza EMC, Pavei C, Ortega GG (2013) Extraction optimization of polyphenols, oxindole alkaloids and quinovic acid glycosides from cat's claw bark by Box-Behnken design. *Ind Crops Prod* 48:153–161. <https://doi.org/10.1016/j.indcrop.2013.04.026>
- Karam M, Petit J, Zimmer D, Baudelaire EB, Djantou EB, Scher J (2016) Effects of drying and grinding in production of fruit and vegetable powders: a review. *J Food Eng* 188:32–49. <https://doi.org/10.1016/j.jfoodeng.2016.05.001>
- Kemp IC, Fyhr BC, Laurent S, Roques MA, Groenewold CE, Tsotsas E, Sereno AA, Bonazzi CB, Bimbenet JJ, Kind M (2001) Methods for processing experimental drying kinetics data. *Drying Technol* 19:15–34. <https://doi.org/10.1081/DRT-100001350>
- Khanlari Y, Aroujalian A, Fazel S, Fathizadeh M (2014) An experimental work and mathematical modeling on kinetic drying of tomato pulp under different modified atmosphere conditions. *Int J Food Prop* 17:1–12. <https://doi.org/10.1080/10942912.2011.576358>
- Kumari P, Khatkar BS (2018) Nutritional composition and drying kinetics of aonla fruits. *J Food Sci Technol* 55:3135–3143. <https://doi.org/10.1007/s13197-018-3241-8>
- Kyi TM, Daud WRW, Mohammad AB, Samsudin MW, Kadhum AAH, Talib MZM (2005) The kinetics of polyphenol degradation during the drying of Malaysian cocoa beans. *Int J Food Sci Technol* 40:323–331
- Lee JH, Rhim J-W (2010) Rehydration kinetics of vacuum-dried *Salicornia herbacea*. *Food Sci Biotechnol* 19:1083–1087. <https://doi.org/10.1007/s10068-010-0152-5>
- Li W, Yuan L, Xiao X, Yang X (2016) Dehydration of kiwifruit (*Actinidia deliciosa*) slices using heat pipe combined with impingement technology. *Int J Food Eng* 12:265–276. <https://doi.org/10.1515/ijfe-2015-0165>
- Liang P, Wang H, Chen C, Ge F, Liu D, Li S, Han B, Xiong X, Zhao S (2013) The use of Fourier Transform Infrared Spectroscopy for quantification of adulteration in virgin walnut oil. *J Spectrosc* 2013:1–6. <https://doi.org/10.1155/2013/305604>
- Lu D, Zhang M, Wang S, Cai J, Zhou X, Zhu C (2010) Nutritional characterization and changes in quality of *Salicornia bigelovii* Torr. during storage. *LWT Food Sci Technol* 43:519–524. <https://doi.org/10.1016/j.lwt.2009.09.021>
- Martynenko A, Bück A (2019) Intelligent control in drying. CRC Press, Boca Raton
- Michailidis PA, Krokida MK (2015) Drying of foods. In: Varzakas T, Tzia C (eds) *Food engineering handbook*. CRC Press, New York, pp 375–435
- Mujumdar AS (2006) *Handbook of industrial drying*. Taylor & Francis, Milton Park
- Nguyen TK, Mondor M, Ratti C (2018) Shrinkage of cellular food during air drying. *J Food Eng* 230:8–17. <https://doi.org/10.1016/j.jfoodeng.2018.02.017>
- Oikonomopoulou VP, Krokida MK (2013) Novel aspects of formation of food structure during drying. *Drying Technol* 31:990–1007. <https://doi.org/10.1080/07373937.2013.771186>
- Patel S (2016) *Salicornia*: evaluating the halophytic extremophile as a food and a pharmaceutical candidate. 3 *Biotech*. <https://doi.org/10.1007/s13205-016-0418-6>
- Poiana M-A, Alexa E, Munteanu M-F, Gligor R, Moigradean D (2015) Use of ATR-FTIR spectroscopy to detect the changes in extra virgin olive oil by adulteration with soybean oil and high temperature heat treatment. *Open Chem* 13:689–698. <https://doi.org/10.1515/chem-2015-0110>
- Rahman MdM, Kim M-J, Kim J-H, Kim S-H, Go HK, Kweon M-H, Kim D-H (2018) Desalted *Salicornia europaea* powder and its active constituent, *trans*-ferulic acid, exert anti-obesity effects by suppressing adipogenic-related factors. *Pharm Biol* 56:183–191. <https://doi.org/10.1080/13880209.2018.1436073>
- Renna M, Gonnella M, Caretto S, Mita G, Serio F (2017) Sea fennel (*Crithmum maritimum* L.): from underutilized crop to new dried product for food use. *Genet Resour Crop Evol* 64:205–216
- Roberts JS, Kidd DR, Padilla-Zakour O (2008) Drying kinetics of grape seeds. *J Food Eng* 89:460–465. <https://doi.org/10.1016/j.jfoodeng.2008.05.030>
- Rodrigues M, Gangadhar K, Vizetto-Duarte C, Wubshet SG, Nyberg NT, Barreira L, Varela J, Custódio L (2014) Maritime halophyte species from southern Portugal as sources of bioactive molecules. *Marine Drugs* 12:2228–2244. <https://doi.org/10.3390/md12042228>
- Rufo L, de la Fuente V, Sanchez-Mata D (2016) *Sarcocornia* plant communities of the Iberian Peninsula and the Balearic Islands. *Phytocoenologia* 46:383–396. <https://doi.org/10.1127/phyto/2016/0113>
- Sacilik K (2007) Effect of drying methods on thin-layer drying characteristics of hull-less seed pumpkin (*Cucurbita pepo* L.). *J Food Eng* 79:23–30. <https://doi.org/10.1016/j.jfoodeng.2006.01.023>
- Said LBH, Najjaa H, Neffati M, Bellagha S (2013) Color, phenolic and antioxidant characteristic changes of *Allium roseum* leaves during drying. *J Food Qual* 36:403–410. <https://doi.org/10.1111/jfq.12055>
- Sansaniwal SK, Kumar M (2015) Analysis of ginger drying inside a natural convection indirect solar dryer: An experimental study. *J Mech Eng Sci* 9:1671–1685. <https://doi.org/10.15282/jmes.9.2015.13.0161>
- Srikiatden J, Roberts JS (2007) Moisture transfer in solid food materials: A review of mechanisms, models, and measurements. *Int J Food Prop* 10:739–777. <https://doi.org/10.1080/10942910601161672>
- Steffen S, Ball P, Mucina L, Kadereit G (2015) Phylogeny, biogeography and ecological diversification of *Sarcocornia* (Salicornioideae, Amaranthaceae). *Ann Bot* 115(3):353–368
- Stuart B (1997) *Biological applications of infrared spectroscopy*. Wiley, Chichester
- Tanongkankit Y, Chiewchan N, Devahastin S (2012) Physicochemical property changes of cabbage outer leaves upon preparation into functional dietary fiber powder. *Food Bioprod Process* 90:541–548. <https://doi.org/10.1016/j.fbp.2011.09.001>

- Tijksens LMM, Schijvens E, Biekman ESA (2001) Modelling the change in colour of broccoli and green beans during blanching. *Innov Food Sci Emerging Technol* 2:303–313
- van Boekel MAJS (1999) Testing of kinetic models: usefulness of the multiresponse approach as applied to chlorophyll degradation in foods. *Food Res Int* 32:261–269. [https://doi.org/10.1016/S0963-9969\(99\)00080-0](https://doi.org/10.1016/S0963-9969(99)00080-0)
- van Boekel MAJS (2000) Kinetic modelling in food science: a case study on chlorophyll degradation in olives. *J Sci Food Agric* 80:3–9. [https://doi.org/10.1002/\(SICI\)1097-0010\(20000101\)80:1%3c3:AID-JSFA532%3e3.0.CO;2-3](https://doi.org/10.1002/(SICI)1097-0010(20000101)80:1%3c3:AID-JSFA532%3e3.0.CO;2-3)
- Vega A, Fito P, Andrés A, Lemus R (2007) Mathematical modeling of hot-air drying kinetics of red bell pepper (var. Lamuyo). *J Food Eng* 79:1460–1466. <https://doi.org/10.1016/j.jfoodeng.2006.04.028>
- Vega-Gálvez A, Andrés A, Gonzalez E, Notte-Cuello E, Chacana M, Lemus-Mondaca R (2009) Mathematical modelling on the drying process of yellow squat lobster (*Cervimunida jhoni*) fishery waste for animal feed. *Anim Feed Sci Technol* 151:268–279. <https://doi.org/10.1016/j.anifeedsci.2009.01.003>
- Ventura Y, Sagi M (2013) Halophyte crop cultivation: the case for *Salicornia* and *Sarcocornia*. *Environ Exp Bot* 92:144–153. <https://doi.org/10.1016/j.envexpbot.2012.07.010>
- Ventura Y, Wuddineh WA, Myrzabayeva M, Alikulov Z, Khozin-Goldberg I, Shpigel M, Samocha TM, Sagi M (2011) Effect of seawater concentration on the productivity and nutritional value of annual *Salicornia* and perennial *Sarcocornia* halophytes as leafy vegetable crops. *Sci Hortic* 128:189–196. <https://doi.org/10.1016/j.scienta.2011.02.001>
- Yang R-L, Li Q, Hu Q-P (2020) Physicochemical properties, microstructures, nutritional components, and free amino acids of *Pleurotus eryngii* as affected by different drying methods. *Sci Rep* 10:1–9. <https://doi.org/10.1038/s41598-019-56901-1>
- Yuan J, Hao L-J, Wu G, Wang S, Duan J, Xie G-Y, Qin M-J (2015) Effects of drying methods on the phytochemicals contents and antioxidant properties of chrysanthemum flower heads harvested at two developmental stages. *J Funct Foods* 19:786–795. <https://doi.org/10.1016/j.jff.2015.10.008>
- Yucel U, Alpas H, Bayindirli A (2010) Evaluation of high pressure pretreatment for enhancing the drying rates of carrot, apple, and green bean. *J Food Eng* 98:266–272. <https://doi.org/10.1016/j.jfoodeng.2010.01.006>
- Zhu T, Row KH (2010) Extraction and determination of  $\beta$ -sitosterol from *Salicornia herbacea* L. using monolithic cartridge. *Chromatographia* 71:981–985. <https://doi.org/10.1365/s10337-010-1574-1>
- Zielinska M, Markowski M (2010) Air drying characteristics and moisture diffusivity of carrots. *Chem Eng Process* 49:212–218. <https://doi.org/10.1016/j.ccep.2009.12.005>

**Publisher's Note** Springer Nature remains neutral with regard to jurisdictional claims in published maps and institutional affiliations.